RSC Advances

ROYAL SOCIETY OF CHEMISTRY

www.rsc.org/advances

Journal Name

RSCPublishing

COMMUNICATION

Cite this: DOI: 10.1039/x0xx00000x

Received ooth January 2012,
Accepted ooth January 2012

DOI: 10.1039/x0xx00000x

www.rsc.org/

Polarization transfer solid-state NMR: A new method for studying cellulose dissolution

S. Gustavsson,[a] L. Alves,[b] B. Lindman,[a,b] and D. Topgaard[a]

Polarization transfer solid-state NMR is shown to give molecular-level information about both dissolved and solid cellulose in aqueous dissolution media with sodium hydroxide or tetrabutylammonium hydroxide, thus paving the way for future studies of the molecular details of cellulose dissolution.

Commercial processes for regeneration of cellulose into fibers and films typically involve dissolution in solvents with toxic components such as carbon disulfide or cupper ions. Rational design of environmentally benign media for cellulose dissolution requires thorough understanding of the forces acting between the cellulose molecules in the solid state, as well as between the cellulose and the components of the dissolution medium.

From an economical and environmental perspective, dissolution media based on water are strongly preferred. Hence, it is of utmost importance to pinpoint the nature of the intermolecular forces responsible for the aqueous insolubility of cellulose. The predominant view has been to attribute the insolubility to extensive hydrogen bonding between adjacent polymer chains in the solid state.[1,2] This view has recently been challenged in the so-called "Lindman hypothesis",[3] instead emphasizing interactions between hydrophobic patches on the cellulose.[4,5] Efficient aqueous dissolution media should consequently contain additives that have the capability to protect the hydrophobic patches from the surrounding water.

Current aqueous dissolution media include additives such as NaOH[6] or tetraalkylammonium salts.[7] Although the literature abounds with speculations about the molecular mechanisms of the dissolution process, often expressed in terms of "breaking the intermolecular hydrogen bonding" or similar phrases,[2,8] direct experimental evidence is still missing. In our opinion, the key for understanding cellulose dissolution is a detailed molecular characterization of partially dissolved cellulose, i.e. the actual dissolution medium with co-existence between solid and dissolved cellulose, during the various stages of the dissolution process.

Solid, dissolved, and regenerated cellulose have been separately investigated with a wide range of experimental techniques: infrared spectroscopy,[9] powder[10] and fiber[11] X-ray diffraction, transmission[12] and scanning[13] electron microscopy, and neutron fiber diffraction[14] to mention just a few. Although they all give useful information about some aspects of the starting material or the final product, neither of them have the ability to extract molecular-level information about both the dissolved and the solid polymer in the actual dissolution medium.

Nuclear magnetic resonance (NMR) has in its high-resolution[15] and solid-state[16] incarnations been applied to both dissolved[17,18] and solid[19,20] cellulose. We have recently suggested an experimental approach dubbed polarization transfer solid-state NMR (PT ssNMR)[21] that combines features of both high-resolution and solid-state NMR, thus enabling studies of all the constituent phases in complex materials with solid, liquid, and liquid crystalline domains. The method has been applied to hydrated surfactants,[21,22] lipid biomembranes,[23] lipid-amyloid fibril aggregates,[24] and intact *stratum corneum*,[25-27] all of which containing amphiphilic molecules in wide a range of physical states. The purpose of this communication is to demonstrate the potential of PT ssNMR for detailed characterization of both the liquid and the solid phases in cellulose dissolution media.

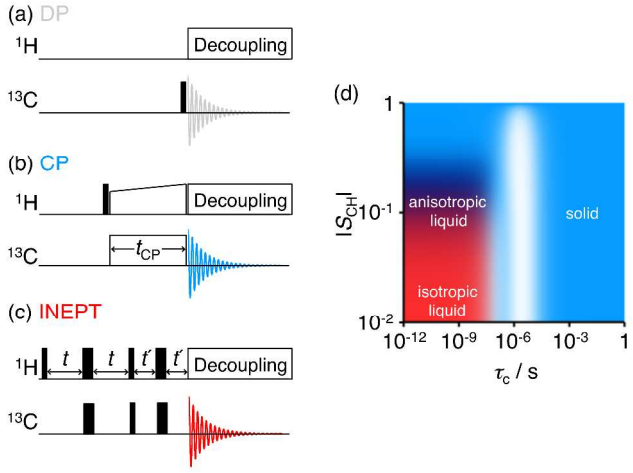

Fig. 1. Polarization transfer solid-state NMR (PT ssNMR). (a-c) NMR pulse sequences with detection of the ^{13}C signal under ^{1}H decoupling and magic-angle spinning (MAS). DP is using the thermal equilibrium polarization of ^{13}C, while CP and INEPT rely on polarization transfer from ^{1}H to ^{13}C. Narrow and broad vertical lines indicate 90° and 180° radiofrequency pulses. (d) Theoretical CP (blue) and INEPT (red) signal enhancement vs. the CH-bond orientational order parameter S_{CH} and reorientational correlation time τ_c. The enhancement factor was calculated for a tertiary carbon atom as described in Nowacka et al.[22] using the experimental parameters of the current study,[†] which were selected to, with least possible ambiguity, discriminate between isotropic liquids (only INEPT), anisotropic liquids (both INEPT and CP), and solids (only CP) according to the labeled areas in panel (d). White indicates lack of signal for both CP and INEPT.

In brief, PT ssNMR gives information about molecular structure, conformation, and packing through the ^{13}C chemical shifts, as well as about molecular dynamics via the signal intensities obtained with the polarization transfer schemes CP (cross polarization)[28] and INEPT (insensitive nuclei enhanced by polarization transfer).[29] The CP and INEPT techniques are traditionally used to boost the signals for solids and liquids, respectively, in comparison to the one available from the ^{13}C direct polarization (DP). Schematics of the pulse sequences that jointly constitute PT ssNMR are displayed in Fig. 1a-c. The ^{13}C signal is acquired under magic-angle spinning (MAS) and high-power ^{1}H decoupling,[30] giving spectra with reasonably high resolution for both liquids and solids. Fig. 1d shows theoretical CP and INEPT efficiencies as a function of the rate and anisotropy of CH-bond reorientation. The DP signal is quantitative, i.e. proportional to the concentration, if the recycle delay is much longer than the longitudinal relaxation time constant T_1, which depends on the molecular dynamics. Under the experimental conditions used here,† our previously developed theoretical model[22] shows that the DP signals are quantitative only if they are accompanied by INEPT, i.e. for isotropic and anisotropic liquids.

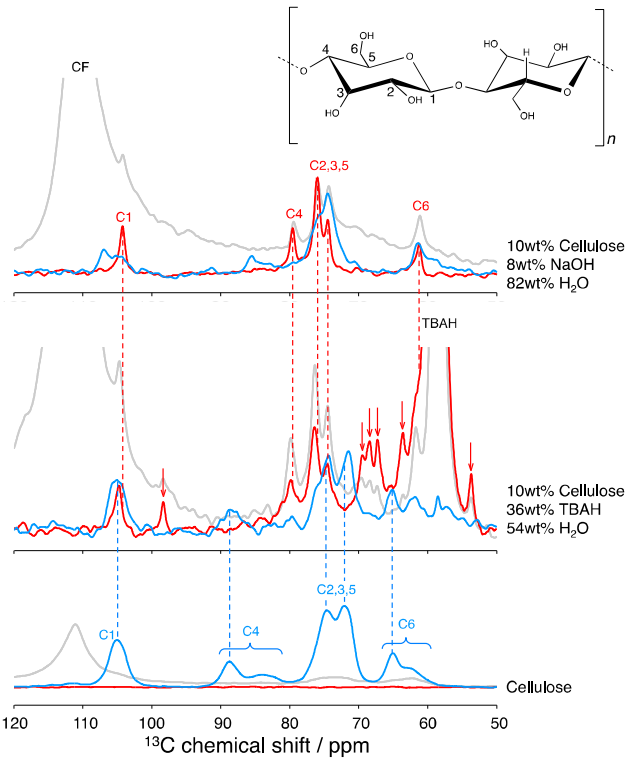

Fig. 2. PT ssNMR data† for microcrystalline cellulose in the initial dry state (bottom), as well as partially dissolved in aqueous TBAH (middle) and NaOH (top). DP, CP, and INEPT spectra are shown in gray, blue, and red, respectively. The assignments of the solid (blue) and dissolved (red) cellulose peaks refer to the carbon atom numbering in the structural formula. The blue and red dashed lines represent literature data for cellulose I in wood pulp fibers[31] and dissolved cellulose,[18] respectively. The labels TBAH and CF point out the truncated peaks from the TBA^+ ions and the Teflon spacer of the MAS rotor, respectively, while the arrows indicate TBA^+ breakdown products. The data was acquired at 25 °C and 125 MHz ^{13}C Larmor frequency with 5 kHz MAS and 88 kHz TPPM ^{1}H decoupling. The spectra are zoomed-in on the 50-120 ppm spectral region relevant for cellulose, and, independently for each sample, magnified to facilitate observation of the cellulose resonance lines.

Table 1. Chemical shifts* of partially dissolved cellulose.

Sample	Fraction	Carbon atom				Comment
		C1	C4	C2,3,5	C6	
Dry	Solid	105.1	88.8	74.6, 72.1	65.0	Cellulose I
TBAH	Solid	105.1	88.7	74.4, 71.5	65.1	Cellulose I
	Dissolved	104.7	79.8	76.4, 74.5	61.7	
NaOH	Solid	107.1	85.6	75.8, 74.6	61.5	Cellulose II
	Dissolved	104.3	79.6	76.0, 74.5	61.3	

*Shifts are given in ppm with α-glycine at 176.03 ppm as external standard. The precision is limited to ±0.2 ppm by the acquisition time.

The experimental PT ssNMR results† are displayed in Fig. 2 and the ^{13}C chemical shifts of the peaks assigned to cellulose are compiled in Table 1. The CP and INEPT spectra are shown with the colors blue and red, respectively, to give an intuitive visual impression of which peaks originate from segments with slow (CP) or fast (INEPT) molecular dynamics. As a reference, the DP spectra are shown in gray. The dry cellulose gives intense CP peaks while INEPT is absent, consistent with cellulose being in a solid state. The observed CP chemical shifts are typical for cellulose I,[32,33] in particular the values 105.4 (C1), 89.1 (C4), 75.3/72.7 (C2,3,5), and 65.5 (C6) ppm for wood pulp fibers[31] having low crystallinity.

The sample with cellulose dissolved in aqueous tetrabutylammonium hydroxide (TBAH) gives signal with both CP and INEPT, showing that it contains both solid and liquid/dissolved components. The similarity between the CP spectra of the dry cellulose and the viscous TBAH solution makes us conclude that the latter contains undissolved residues of the cellulose I starting material. The INEPT spectrum comprises a multitude of peaks, the most prominent originating from the four inequivalent carbons of the TBA^+ ion. Only one of these peaks is located within the spectral window shown in Fig. 2. The remaining INEPT peaks are assigned to dissolved cellulose, as well as to tributylamine and 1-butene which are formed from the TBA^+ ions by Hofmann elimination.[34] The chemical shifts of the dissolved cellulose in the dissolution medium are similar to literature data for ultra-centrifuged samples of regenerated cellulose dissolved in 10 wt% NaOH(aq): 104.7 (C1), 79.9 (C4), 76.4/75.0 (C2,3,5), and 61.9 (C6) ppm.[18] According to the theoretical calculations in Fig. 1d, the presence of INEPT peaks for the cellulose implies that the CH-bonds reorient on a time-scale faster than 100 ns, which in turn is a strong indication that the cellulose is molecularly dissolved. Comparison between the areas of the DP peaks from dissolved cellulose, TBA^+, and tributylamine shows that the fraction of TBA^+ breakdown is about 4.9%, while the molar ratio between the tributylamine and the glucose units of the dissolved cellulose is approximately 11%.

Also the NaOH(aq) solution gives both CP and INEPT signals. While the INEPT peaks are similar to the ones assigned to dissolved cellulose in the TBAH(aq) sample, the CP peaks are noticeably different. Comparison with literature data[32,35] indicates that the solid fraction is cellulose II, which is typical for regenerated cellulose. The absence of cellulose I resonance lines, in particular the distinct C6 line at 65 ppm, shows that all the original cellulose I has been dissolved and some of it later precipitated as cellulose II.

Here we have shown that both the solid and the dissolved cellulose components can be detected with PT ssNMR applied to the actual dissolution medium. These results form the basis for future studies of the mechanisms of cellulose dissolution, and it is thus pertinent to suggest a few properties about which PT ssNMR could give useful information. Although neither CP

nor INEPT yields truly quantitative data, comparison between their areas at least give a rough order-of-magnitude estimate of the ratio between the solid and dissolved fractions, and growth of one type of peak at the expense of the other is an indication that the ratio is changing. Comparison between the DP, CP, and INEPT intensities give qualitative information on molecular dynamics.[22,26] Changes in properties such as molecular conformation and interactions with surrounding molecules and ions in the solution can be followed by observation of the precise values of the chemical shifts. The presence of minor amounts of dissolved impurities can be readily detected in the DP and INEPT spectra. In the TBAH(aq) case, the impurities result from chemical degradation of the major components, and are thus difficult to avoid. Considering the suggested importance of hydrophobic interactions in cellulose systems,[5] the effects of such unintentional hydrophobic or amphiphilic co-solutes must be taken into account in any attempt of rationalizing the observed cellulose solubility in terms of intermolecular interactions between the components of the system.

This work was financially supported by the Crafoord foundation, Södra Skogsägarnas Stiftelse, Stiftelsen Nils och Dorthi Troëdssons forskningsfond, the Swedish Research Council (VR, projects 2009-6794 and 2011-4334), and the Portuguese Foundation for Science and Technology (FCT, project PTDC/AGR-TEC/4049/2012). Alexander Idström (Chalmers University of Technology, Sweden) is gratefully acknowledged for discussions about the ^{13}C spectra of the solid cellulose polymorphs.

Notes and references

[a] Division of Physical Chemistry, Department of Chemistry, Lund University, Lund, Sweden.

[b] Department of Chemistry, University of Coimbra, Coimbra, Portugal.

† Samples were prepared by adding microcrystalline cellulose (Avicel PH 101 from Sigma Aldrich, DP = 260) to aqueous solutions with 8.9 wt% NaOH or 40 wt% tetrabutylammonium hydroxide (TBAH), under stirring, giving final cellulose concentrations of 10 wt%. Solutions of cellulose in NaOH were stored at -18 ºC for 2 h and then kept at room temperature. The resulting clear and visually homogeneous viscous solutions were transferred with a syringe to 4 mm HR-MAS rotors (Bruker, Germany) specifically designed for retaining liquids during MAS. NMR experiments were performed at 25 ºC on a Bruker AVII-500 spectrometer operating at ^{1}H and ^{13}C Larmor frequencies of 500 and 125 MHz, respectively, with a 4 mm ^{13}C/^{31}P/^{1}H E-free probe (Bruker, Germany). PT ssNMR data was recorded with the pulse sequences in Fig. 1a-c using 5 kHz MAS, 88 kHz TPPM decoupling,[36] 20 ms acquisition time, 300 ppm spectral width, and 80 kHz nutation frequency for 90º and 180º pulses. CP was performed with t_{CP} = 1 ms, 80 kHz ^{13}C nutation frequency, and linear ramp[37] from 72 to 88 kHz ^{1}H nutation frequency. The time delays for refocused INEPT[38] were □ = 1.8 ms and □′ = 1.2 ms. Each spectrum was recorded by accumulating 3072 transient with 5 s recycle delay, giving a measurement time of 12.5 h per sample. The time-domain data was zero-filled from 755 to 8192 complex points, Fourier transformed with 100 Hz line broadening, automatically phase corrected,[39] and baseline corrected using customized Matlab scripts based on matNMR.[40]

1. R. Bodvik, A. Dedinaite, L. Karlson, M. Bergström, P. Bäverbäck, J. S. Pedersen, K. Edwards, G. Karlsson, I. Varga and P. M. Claesson, *Colloids Surf. A*, 2010, **354**, 162-171.
2. L. Zhang, D. Ruan and S. Gao, *J. Polym. Sci. B Polym. Phys.*, 2002, **40**, 1521-1529.
3. W. G. Glasser, R. H. Atalla, J. Blackwell, R. M. Brown Jr., W. Burchard, A. D. French, D. O. Klemm, P. Navard and Y. Nishiyama, *Cellulose*, 2012, **19**, 589-598.
4. B. Lindman, G. Karlström and L. Stigsson, *J. Mol. Liq.*, 2010, **156**, 76-81.
5. B. Medronho, A. Romano, M. G. Miguel, L. Stigsson and B. Lindman, *Cellulose*, 2012, **19**, 581-587.
6. A. Isogai and R. H. Atalla, *Cellulose*, 1998, **5**, 309-319.
7. N. Sun, M. Rahman, Y. Qin, M. L. Maxim, H. Rodríguez and R. D. Rogers, *Green Chem.*, 2009, **11**, 646-655.
8. M. Abe, Y. Fukaya and H. Ohno, *Chem. Commun.*, 2012, **48**, 1808-1810.
9. N. Labbé, T. G. Rials, S. S. Kelley, Z.-M. Cheng, J.-Y. Kim and Y. Li, *Wood Sci. Technol.*, 2005, **39**, 61-76.
10. P. Mansikkamäki, M. Lahtinen and K. Rissanen, *Cellulose*, 2005, **12**, 233-242.
11. P. Langan, Y. Nishiyama and H. Chanzy, *Biomacromolecules*, 2001, **2**, 410-416.
12. N. Luo, Y. Lv, D. Wang, J. Zhang, J. Wu, J. He and J. Zhang, *Chem. Commun.*, 2012, **48**, 6283-6285.
13. T.-Q. Li, U. Henriksson, T. Klason and L. Ödberg, *J. Colloid Interface Sci.*, 1992, **154**, 305-315.
14. M. Wada, Y. Nishiyama, G. Bellesia, T. Forsyth, S. Gnanakaran and P. Langan, *Cellulose*, 2011, **18**, 191-206.
15. J. Keeler, *Understanding NMR spectroscopy*, Wiley, 2005.
16. M. Duer, *Introduction to solid-state NMR spectroscopy*, Blackwell Publishing Ltd, Oxford, 2004.
17. J. C. Gast, R. H. Atalla and R. D. McKelvey, *Carbohydr. Res.*, 1980, **84**, 137-146.
18. K. Kamide, K. Okajima, T. Matsui and K. Kowsaka, *Polymer J.*, 1984, **16**, 857-866.
19. W. L. Earl and D. L. VanderHart, *Macromolecules*, 1981, **14**, 570-574.
20. R. H. Atalla and D. L. VanderHart, *Solid State Nucl. Magn. Reson.*, 1999, **15**, 1-19.
21. A. Nowacka, P. C. Mohr, J. Norrman, R. W. Martin and D. Topgaard, *Langmuir*, 2010, **26**, 16848-16856.
22. A. Nowacka, N. A. Bongartz, O. H. S. Ollila, T. Nylander and D. Topgaard, *J. Magn. Reson.*, 2013, **230**, 165-175.
23. A. Nowacka, S. Douezan, L. Wadsö, D. Topgaard and E. Sparr, *Soft Matter*, 2012, **8**, 1482-1491.
24. E. Hellstrand, A. Nowacka, D. Topgaard, S. Linse and E. Sparr, *PLOS ONE*, 2013, **8**, e77235.
25. S. Björklund, T. Ruzgas, A. Nowacka, I. Dahi, D. Topgaard, E. Sparr and J. Engblom, *Biophys. J.*, 2013, **104**, 2639-2650.
26. S. Björklund, A. Nowacka, J. A. Bouwstra, E. Sparr and D. Topgaard, *PLOS ONE*, 2013, **8**, e61889.
27. S. Björklund, J. M. Andersson, A. E. Nowacka, Q. D. Pham, D. Topgaard and E. Sparr, *Soft Matter*, Accepted.
28. A. Pines, J. S. Waugh and M. G. Gibby, *J. Chem. Phys.*, 1972, **56**, 1776-1777.
29. G. A. Morris and R. Freeman, *J. Am. Chem. Soc.*, 1979, **101**, 760-762.
30. J. Schaefer, E. O. Stejskal and R. Buchdahl, *Macromolecules*, 1975, **8**, 291-296.
31. K. Kamide, K. Okajima, K. Kowsaka and T. Matsui, *Polymer J.*, 1985, **17**, 701-706.
32. D. L. VanderHart and R. H. Atalla, *Macromolecules*, 1984, **17**, 1465-1472.
33. H. Kono, T. Erata and M. Takai, *Macromolecules*, 2003, **36**, 5131-5138.
34. M. E. Bos, in *Encyclopedia of Reagents for Organic Synthesis*, ed. L. Paquette, 2004.
35. H. Kono, Y. Numata, T. Erata and M. Takai, *Macromolecules*, 2004, **37**, 5310-5316.
36. A. E. Bennett, C. M. Rienstra, M. l. Auger, K. V. Lakshmi and R. G. Griffin, *J. Chem. Phys.*, 1995, **103**, 6951-6958.
37. G. Metz, X. Wu and S. O. Smith, *J. Magn. Reson. A*, 1994, **110**, 219-227.
38. O. W. Sørensen and R. R. Ernst, *J. Magn. Reson.*, 1983, **51**, 477-489.
39. L. Chen, Z. Weng, L. Goh and M. Garland, *J. Magn. Reson.*, 2002, **158**, 164-168.
40. J. D. van Beek, *J. Magn. Reson.*, 2007, **187**, 19-26.

Detailed molecular-level information on dissolved and solid cellulose in aqueous dissolution media with ionic liquids by Polarization Transfer solid-state NMR.

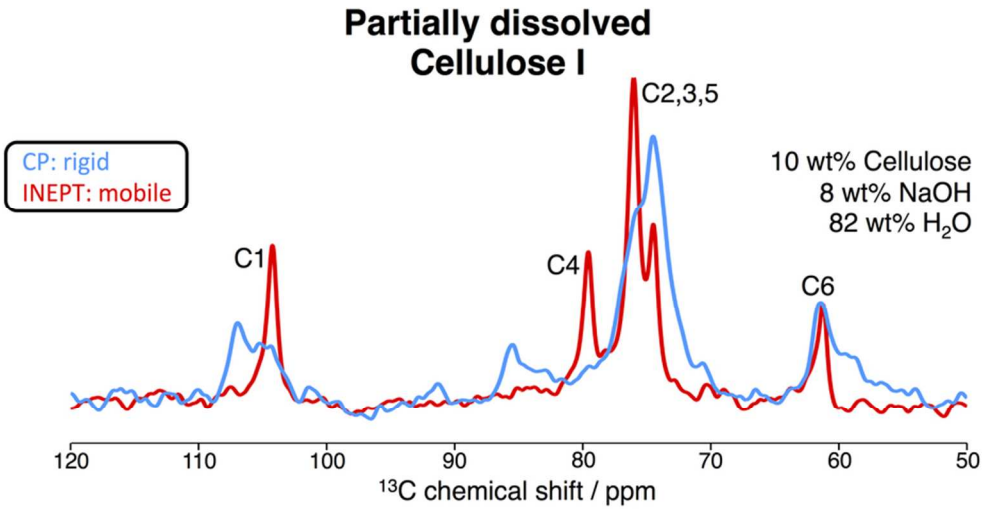

39x19mm (600 x 600 DPI)